Secure outage probability of cognitive radio network relying non-orthogonal multiple access scheme

Chi-Bao Le, Dinh-Thuan Do
Faculty of Electronics Technology, Industrial University of Ho Chi Minh City (IUH), Ho Chi Minh City, Vietnam

Article Info

Article history:

Received Oct 16, 2020
Revised Jan 7, 2021
Accepted Feb 16, 2021

Keywords:

Cognitive radio
NOMA
Secure outage probability

ABSTRACT

This paper studies the secondary network relying relay selection to transmit signal from the secondary source (base station) to two destinations. Especially, two destinations are required non-orthogonal multiple access (NOMA) scheme and it benefits to implementation of the Internet of Things (IoT) systems. However, eavesdropper overhears signal related link from selected relay to destination. This paper measure secure performance via metric, namely secure outage probability (SOP). In particular, signal to noise ratio (SNR) criterion is used to evalute SOP to provide reliable transmission to the terminal node. Main results indicates that the considered scheme provides performance gap among two signals at destination. The exactness of derived expressions is confirmed via numerical simulation.

Corresponding Author:

Dinh-Thuan Do
Faculty of Electronics Technology
Industrial University of Ho Chi Minh City
12 Nguyen Van Bao Road, Go Vap District, Ho Chi Minh City, Vietnam
Email: dodinhthuan@iuh.edu.vn

1. INTRODUCTION

Recently, spectrum occupation results in lack of resource, and cognitive radio (CR) is introduced as technique to provide network with higher the spectrum efficiency. In CR, users in the secondary network are able to dynamically access the licensed spectrum provided by primary network [1-3]. In the current researches about the cognitive radio networks, two popular kinds of CR network are employed, such as underlay and/or overlay spectrum sharing strategies. The unused licensed spectrum is reused by secondary users to access network and collision is prohibited with the primary transmission, and such is called as the overlay strategy [4-6]. By controlling the interfere to the primary receivers under a threshold, the secondary network applying the underlay strategy, and it then shares with the primary users in term of licensed spectrum. Advantages of CR can be determined in various works such as [7-9].

To further improve the spectrum efficiency, non-orthogonal multiple access (NOMA) technique is also introduced, it benefits to wireless network by allocating multiple users using different levels of transmit power to access the same frequency [10-12]. The receiver need to distinguish the different signals, and it requires operation of successive interference cancellation (SIC) [12]. The NOMA based CR networks are studied recently. Taking advantages of both the cognitive radio and NOMA techniques, it will benefit from the spectrum efficiency and massive users connected [13].

It is necessary to put our concerns on information security for the cognitive radio networks in which NOMA is activated. Advantage of spectrum sharing nature in the cognitive radio benefits to CR-NOMA networks, however it is vulnerable to be eavesdropped since the eavesdropper can pretend to be a secondary user.

Recently, secure performance is presented in the context of NOMA implementation [15-24]. Motivated by these papers, we consider secure outage probability of CR-NOMA.

2. SYSTEM MODEL

In Figure 1, the considered system contains secondary network including base station BS, and N relay nodes, two destination U_1, U_2, one eavesdropper E, We denote h_u as channel dedicating to node u, and it follows Rayleigh fading model with channel gain λ_u. It is noted that P_S is transmit power at BS and it is limited under constraint with the primary network. The interference channel from BS to the primary network is h_{SP}.

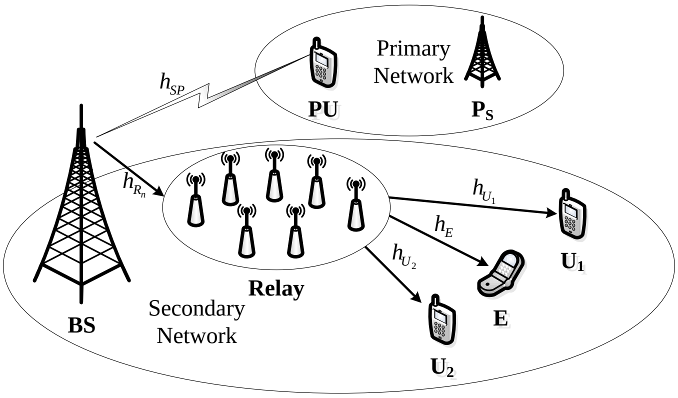

Figure 1. System model of CR-NOMA with eavesdropper

The transmit power constraint is limited at BS

$$P_S \leq \min\left(\frac{I}{|h_{SP}|^2}, \bar{P}_S\right) \tag{1}$$

where $\bar{P}_S$ and I is maximum average transmit power at the BS and interference temperature constraint (ITC) at primary destination P_D.

In the first time, R receives the following signal

$$y_R = h_{R_n}\left(\sqrt{a_1 P_S}x_1 + \sqrt{a_2 P_S}x_2\right) + n_{R_n} \tag{2}$$

where h_{R_n} is the channel between BS and R, the AWGN noise terms at R is n_{R_n} indicates. To decode signal x_1 and x_2 at R, the signal-to-interference-plus-noise ratio (SINR) and signal-to-noise ratio (SNR) can be respectively written as (3)

$$\gamma_R^1 = \frac{a_1\rho_S|h_{R_n}|^2}{a_2\rho_S|h_{R_n}|^2 + 1} \tag{3}$$

where $\rho_S = \frac{P_S}{\sigma^2}$ is the transmit SNR at the BS.

At relay relying SIC, the received SINR at R to detect its own message x_2 is given by (4).

$$\gamma_R^2 = a_2\rho_S|h_{Rn}|^2 \tag{4}$$

In the next phase, signal $\sqrt{a_1 P_R}\bar{x}_1 + \sqrt{a_2 P_R}\bar{x}_2$ is forwarded by relay R to $U_i, i = 1, 2$. We denote P_R is the transmit power at R. U_i receives the following signal

$$y_{U_i} = h_{U_i}\left(\sqrt{a_1 P_R}\bar{x}_1 + \sqrt{a_2 P_R}\bar{x}_2\right) + n_{U_i} \quad ,\forall i \in \{1,2\} \tag{5}$$

in which the AWGN noise terms is n_{U_i} measured at U_i. h_{R_n} is denoted as the channel between Relay and U_i. Further, principle of NOMA applied to U_i with higher power factor, it can detect $\bar{x}_1$ by considering $\bar{x}_2$ as a background noise with the following SINR

$$\gamma_{U_1} = \frac{a_1 \rho_R |h_{U_1}|^2}{a_2 \rho_R |h_{U_1}|^2 + 1} \tag{6}$$

where $\rho_R = \frac{P_R}{\sigma^2}$ is the transmit SNR at R.

To continue detecting procedure, U_2 needs SIC to decode $\bar{x}_1$ while considering its own data $\bar{x}_2$ as a noise. The SINR is written as (7).

$$\gamma_{U_2,x_1} = \frac{a_1 \rho_R |h_{U_2}|^2}{a_2 \rho_R |h_{U_2}|^2 + 1} \tag{7}$$

In this regard, U_2 detects its own signal and the corresponding SNR is given as (8).

$$\gamma_{U_2,x_2} = a_2 \rho_R |h_{U_2}|^2 \tag{8}$$

Unfortunately, eavesdropper steals information from the selected relay, the received signal at E is given as (9)

$$y_E = h_E\left(\sqrt{a_1 P_E}\bar{x}_1 + \sqrt{a_2 P_E}\bar{x}_1\right) + n_E \tag{9}$$

where n_E is the AWGN noise terms at E. The channel between Relay and E is h_E. Then, SNR at E is given as

$$\gamma_{Ei} = a_i \rho_E |h_E|^2 \quad , i \in \{1,2\} \tag{10}$$

where $\rho_E = \frac{P_E}{\sigma^2}$ is transmit SNR at E.

The secrecy capacity for U_1 is computed as (11).

$$C_1 = \left[\frac{1}{2}\log_2\left(\frac{1 + \min\left(\gamma_R^1, \gamma_{U_1}\right)}{1 + \gamma_{E_1}}\right)\right]^+ \tag{11}$$

where $[x]^+ = \max[x,0]$.

Similarly, the secrecy capacity for U_2 is formulated as (12).

$$C_2 = \left[\frac{1}{2}\log_2\left(\frac{1 + \min\left(\gamma_R^2, \gamma_{U_2,x_2}\right)}{1 + \gamma_{E_2}}\right)\right]^+ \tag{12}$$

The criteria to select relay n^* is defined related the best channel given as (13).

$$n^* = \arg \underbrace{\max}_{1,2,\ldots,N} |h_{R_n}|^2 \tag{13}$$

3. SECRECY PERFORMANCE ANALYSIS

3.1. Secrecy outage probability of U_1

SOP performance at user U_1 is computed by (14)

$$\begin{aligned} P_1^{SOP} &= \Pr\left(C_1 < R_1\right) \\ &= \Pr\left(\frac{1+\min\left(\gamma_R^1, \gamma_{U_1}\right)}{1+\gamma_{E_1}} < 2^{2R_1}\right) \\ &= \Pr\left(\frac{1+\min\left(\frac{a_1\rho_S|h_{R_{n^*}}|^2}{a_2\rho_S|h_{R_{n^*}}|^2+1}, \frac{a_1\rho_R|h_{U_1}|^2}{a_2\rho_R|h_{U_1}|^2+1}\right)}{1+a_1\rho_E|h_E|^2} < 2^{2R_1}\right) \\ &= \Pr\left(\min\left(\frac{a_1\rho_S|h_{R_{n^*}}|^2}{a_2\rho_S|h_{R_{n^*}}|^2+1}, \frac{a_1\rho_R|h_{U_1}|^2}{a_2\rho_R|h_{U_1}|^2+1}\right) < \theta|h_E|^2+\omega_1\right) \end{aligned} \tag{14}$$

where $\theta = 2^{2R_1}a_1\rho_E$ and $\omega_1 = 2^{2R_1}-1$ Next, P_1^{SOP} is rewritten as (15).

$$\begin{aligned} P_1^{SOP} =& 1 - \underbrace{\Pr\left(\frac{a_1\rho_S|h_{R_{n^*}}|^2}{a_2\rho_S|h_{R_{n^*}}|^2+1} > \theta|h_E|^2+\omega_1\right)}_{A} \\ & \times \underbrace{\Pr\left(\frac{a_1\rho_R|h_{U_1}|^2}{a_2\rho_R|h_{U_1}|^2+1} > \theta|h_E|^2+\omega_1\right)}_{B} \end{aligned} \tag{15}$$

We continue compute each component as (16) and (17)

$$\begin{aligned} A =& \underbrace{\Pr\left(|h_{R_{n^*}}|^2 \geq \frac{\left(\theta|h_E|^2+\omega_1\right)}{a_1\bar{\rho}_S - \left(\theta|h_E|^2+\omega_1\right)a_2\bar{\rho}_S}, \bar{\rho}_S < \frac{\rho_I}{|h_{SP}|^2}\right)}_{A_1} \\ & + \underbrace{\Pr\left(|h_{R_{n^*}}|^2 \geq \frac{\left(\theta|h_E|^2+\omega_1\right)|h_{SP}|^2}{\left(a_1 - \left(\theta|h_E|^2+\omega_1\right)a_2\right)\rho_I}, \bar{\rho}_S > \frac{\rho_I}{|h_{SP}|^2}\right)}_{A_2} \end{aligned} \tag{16}$$

$$\begin{aligned} A_1 =& \Pr\left(|h_{R_{n^*}}|^2 \geq \frac{\theta|h_E|^2+\omega_1}{\bar{\rho}_S\left(a_1 - |h_E|^2\theta a_2 - \omega_1 a_2\right)}, |h_E|^2 < \psi, |h_{SP}|^2 < \frac{\rho_I}{\bar{\rho}_S}\right) \\ =& \int_0^{\frac{\rho_I}{\bar{\rho}_S}} f_{|h_{SP}|^2}(x) \int_0^{\psi} f_{|h_E|^2}(y)\left[1 - F_{|h_{R_{n^*}}|^2}\left(\frac{\theta y+\omega_1}{\bar{\rho}_S\left(a_1 - y\theta a_2 - \omega_1 a_2\right)}\right)\right]dxdy \\ =& \left(1 - e^{-\frac{\rho_I}{\bar{\rho}_S\lambda_{SP}}}\right)\sum_{n=1}^{N}\binom{N}{n}\frac{(-1)^{n-1}}{\lambda_E}\int_0^{\psi} e^{-\frac{n(\theta y+\omega_1)}{\lambda_{SR}\bar{\rho}_S(a_1-\theta a_2 y - a_2\omega_1)} - \frac{y}{\lambda_E}}dy \end{aligned} \tag{17}$$

where $\psi = \frac{a_1 - \omega_1 a_2}{a_2 \theta}$. Let $t = 2y/\psi - 1 \Rightarrow y = (t+1)\psi/2 \Rightarrow dy = \psi/2dt$, A_1 is given by (18).

$$\begin{aligned} A_1 = &\left(1 - e^{-\frac{\rho_I}{\bar{\rho}_S \lambda_{SP}}}\right) \sum_{n=1}^{N} \left(\begin{array}{c} N \\ n \end{array} \right) \frac{\psi(-1)^{n-1}}{2\lambda_E} \\ &\times \int_{-1}^{1} e^{-\frac{(t+1)\psi}{2\lambda_E} - \frac{n[\theta\psi(t+1)+2\omega_1]}{\lambda_{SR}\bar{\rho}_S[2a_1 - \theta a_2(t+1)\psi - 2a_2\omega_1]}} dt \end{aligned} \tag{18}$$

Since it is difficult to derive a closed-form expression for (18), an accurate approximation can be achieved for it. Using Gaussian-Chebyshev quadrature, we have (19)

$$A_1 \approx \left(1 - e^{-\frac{\rho_I}{\bar{\rho}_S \lambda_{SP}}}\right) \sum_{n=1}^{N} \sum_{p=1}^{P} \left(\begin{array}{c} N \\ n \end{array} \right) \frac{\psi\pi(-1)^{n-1}\sqrt{1-\xi_p^2}}{2P\lambda_E} e^{-g(\xi_p)} \tag{19}$$

where $\psi = \frac{a_1 - \omega_1 a_2}{a_2 \theta}$, $\xi_p = \cos\left(\frac{2p-1}{2P}\pi\right)$ and $g(x) = \frac{(t+1)\psi}{2\lambda_E} + \frac{n[\theta\psi(t+1)+2\omega_1]}{\lambda_{SR}\bar{\rho}_S[2a_1 - \theta a_2(t+1)\psi - 2a_2\omega_1]}$.
Next, A_2 is calculated as (20)

$$\begin{aligned} A_2 = &\Pr\left(|h_{R_{n^*}}|^2 \geq \frac{\left(\theta|h_E|^2 + \omega_1\right)|h_{SP}|^2}{\left(a_1 - |h_E|^2\theta a_2 - \omega_1 a_2\right)\rho_I}, |h_E|^2 < \psi, |h_{SP}|^2 > \frac{\rho_I}{\bar{\rho}_S} \right) \\ = &\int_0^{\psi} f_{|h_E|^2}(x) \int_{\frac{\rho_I}{\bar{\rho}_S}}^{\infty} f_{|h_{SP}|^2}(y) \left[1 - F_{|h_{Rn^*}|^2}\left(\frac{(\theta x + \omega_1)y}{(a_1 - \theta a_2 x - a_2\omega_1)\rho_I}\right)\right] dxdy \end{aligned} \tag{20}$$

then, A_2 is calculated as (21).

$$\begin{aligned} A_2 = &\sum_{n=1}^{N} \left(\begin{array}{c} N \\ n \end{array} \right) \frac{(-1)^{n-1}}{\lambda_{SP}\lambda_E} \int_0^{\psi} e^{-\frac{x}{\lambda_E}} \int_{\frac{\rho_I}{\bar{\rho}_S}}^{\infty} e^{-y\left(\frac{1}{\lambda_{SP}} + \frac{n(\theta x + \omega_1)}{(a_1 - \theta a_2 x - a_2\omega_1)\rho_I\lambda_{SR}}\right)} dxdy \\ = &\sum_{n=1}^{N} \left(\begin{array}{c} N \\ n \end{array} \right) \frac{(-1)^{n-1}}{\lambda_{SP}\lambda_E} \int_0^{\psi} e^{-\frac{x}{\lambda_E}} \left(\frac{1}{\lambda_{SP}} + \frac{n(\theta x + \omega_1)}{(a_1 - \theta a_2 x - a_2\omega_1)\rho_I\lambda_{SR}}\right)^{-1} \\ &\times e^{-\frac{\rho_I}{\bar{\rho}_S}\left(\frac{1}{\lambda_{SP}} + \frac{n(\theta x + \omega_1)}{(a_1 - \theta a_2 x - a_2\omega_1)\rho_I\lambda_{SR}}\right)} dx \end{aligned} \tag{21}$$

Let $t = 2x/\psi - 1 => x = (t+1)\psi/2 \Rightarrow dx = \psi/2dt$, A_2 is given by (22).

$$\begin{aligned} A_2 = &\sum_{n=1}^{N} \left(\begin{array}{c} N \\ n \end{array} \right) \frac{\psi(-1)^{n-1}}{2\lambda_{SP}\lambda_E} \int_{-1}^{1} e^{-\frac{(t+1)\psi}{2\lambda_E} - \frac{\rho_I}{\bar{\rho}_S}\left(\frac{1}{\lambda_{SP}} + \frac{n(\theta(t+1)\psi + 2\omega_1)}{[2a_1 - \theta a_2(t+1)\psi - 2a_2\omega_1]\rho_I\lambda_{SR}}\right)} \\ &\times \left(\frac{1}{\lambda_{SP}} + \frac{n(\theta(t+1)\psi + 2\omega_1)}{(2a_1 - \theta a_2(t+1)\psi - 2a_2\omega_1)\rho_I\lambda_{SR}}\right)^{-1} dx \end{aligned} \tag{22}$$

Although, it is difficult to derive a closed-form expression for (22), we can obtain an accurate approximation for it. Using Gaussian-Chebyshev quadrature, it can be obtained that

$$A_2 \approx \sum_{n=1}^{N} \sum_{v=1}^{V} \left(\begin{array}{c} N \\ n \end{array} \right) \frac{\psi\pi(-1)^{n-1}\sqrt{1-\zeta_v^2}}{2V\lambda_{SP}\lambda_E\Xi(\zeta_v)} e^{-\frac{(\zeta_v+1)\psi}{2\lambda_E} - \frac{\rho_I\Xi(\zeta_v)}{\bar{\rho}_S}} \tag{23}$$

where $\zeta_v = \cos\left(\frac{2v-1}{2V}\pi\right)$ and $\Xi\left(x\right) = \left(\frac{1}{\lambda_{SR}} + \frac{n(\theta(x+1)\psi+2\omega_1)}{[2a_1-\theta a_2(x+1)\psi-2a_2\omega_1]\rho_I\lambda_{SR}}\right)$.

Substituting (23) and (19) to (16), A is given by (24).

$$\begin{aligned} A \approx & \left(1-e^{-\frac{\rho_I}{\bar{\rho}_S\lambda_{SP}}}\right)\sum_{n=1}^{N}\sum_{p=1}^{P}\binom{N}{n}\frac{\psi\pi(-1)^{n-1}\sqrt{1-\xi_p^2}}{2P\lambda_E}e^{-g(\xi_p)} \\ & +\sum_{n=1}^{N}\sum_{v=1}^{V}\binom{N}{n}\frac{\psi\pi(-1)^{n-1}\sqrt{1-\zeta_v^2}}{2V\lambda_{SP}\lambda_E\Xi\left(\zeta_v\right)}e^{-\frac{(\zeta_v+1)\psi}{2\lambda_E}-\frac{\rho_I\Xi(\zeta_v)}{\bar{\rho}_S}} \end{aligned} \tag{24}$$

Next, B is calculated as (25).

$$\begin{aligned} B = & \Pr\left(\frac{a_1\rho_R{|h_{U_1}|}^2}{a_2\rho_R{|h_{U_1}|}^2+1} > \theta{|h_E|}^2+\omega_1\right) \\ = & \Pr\left({|h_{U_1}|}^2 > \frac{\theta{|h_E|}^2+\omega_1}{\rho_R\left(a_1-{|h_E|}^2\theta a_2-\omega_1 a_2\right)}{|h_E|}^2 < \psi\right) \\ = & \int_0^{\psi} f_{|h_E|^2}\left(x\right)\left[1-F_{{|h_{U_1}|}^2}\left(\frac{\theta x+\omega_1}{\rho_R\left(a_1-x\theta a_2-\omega_1 a_2\right)}\right)\right]dx \\ = & \frac{1}{\lambda_E}\int_0^{\psi} e^{-\frac{x}{\lambda_E}-\frac{\theta x+\omega_1}{\lambda_{U_1}\rho_R(a_1-x\theta a_2-\omega_1 a_2)}}dx \end{aligned} \tag{25}$$

The similar, using Gaussian-Chebyshev quadrature, B is given by (26).

$$B \approx \frac{\psi\pi}{2\lambda_E Q}\sum_{q=1}^{Q}\sqrt{1-\zeta_q^2}e^{-\frac{\psi(\zeta_q+1)}{2\lambda_E}-\frac{\theta\psi(\zeta_q+1)+2\omega_1}{\lambda_{U_1}\rho_R[2a_1-\psi(u+1)\theta a_2-2\omega_1 a_2]}} \tag{26}$$

where $\zeta_q = \cos\left(\frac{2q-1}{2Q}\pi\right)$.

Finally, substituting (26) and (24) to (15), P_1^{SOP} is given by (27).

$$\begin{aligned} P_1^{SOP} = & 1-\left\{\left[\left(1-e^{-\frac{\rho_I}{\bar{\rho}_S\lambda_{SP}}}\right)\sum_{n=1}^{N}\sum_{p=1}^{P}\binom{N}{n}\frac{\psi\pi(-1)^{n-1}\sqrt{1-\xi_p^2}e^{-g(\xi_p)}}{2P\lambda_E}\right.\right. \\ & \left.+\sum_{n=1}^{N}\sum_{v=1}^{V}\binom{N}{n}\frac{\psi\pi(-1)^{n-1}\sqrt{1-\zeta_v^2}}{2V\lambda_{SP}\lambda_E\Xi\left(\zeta_v\right)}e^{-\frac{(\zeta_v+1)\psi}{2\lambda_E}-\frac{\rho_I\Xi(\zeta_v)}{\bar{\rho}_S}}\right] \\ & \left.\times\frac{\psi\pi}{2\lambda_E Q}\sum_{q=1}^{Q}\sqrt{1-\zeta_q^2}e^{-\frac{\psi(\zeta_q+1)}{2\lambda_E}-\frac{\theta\psi(\zeta_q+1)+2\omega_1}{\lambda_{U_1}\rho_R[2a_1-\psi(u+1)\theta a_2-2\omega_1 a_2]}}\right\} \end{aligned} \tag{27}$$

Let $\rho_S \to \infty$, $P_1^{SOP,\infty}$ is given by (28).

$$\begin{aligned} P_1^{SOP,\infty} = & 1-\sum_{n=1}^{N}\sum_{v=1}^{V}\sum_{q=1}^{Q}\binom{N}{n}\frac{\psi^2\pi^2(-1)^{n-1}\sqrt{1-\zeta_q^2}\sqrt{1-\zeta_v^2}}{4VQ\lambda_{SP}\lambda_E^2\Xi\left(\zeta_v\right)} \\ & \times e^{-\frac{(\zeta_v+1)\psi}{2\lambda_E}-\frac{\psi(\zeta_q+1)}{2\lambda_E}} \end{aligned} \tag{28}$$

3.2. Secrecy outage probability of U_2

In similar way, SOP performance at user U_2 is expressed by (29)

$$\begin{aligned} P_2^{SOP} &= \Pr\left(C_2 < R_2\right) \\ &= \Pr\left(\frac{1}{2}\log_2\left(\frac{1+\min\left(\gamma_R^2, \gamma_{U_2,x_2}\right)}{1+\gamma_{E2}}\right) < R_2\right) \\ &= \Pr\left(\min\left(a_2\rho_S|h_{R_{n^*}}|^2, a_2\rho_R|h_{U_2}|^2\right) < \vartheta|h_E|^2+\omega_2\right) \\ &= 1-\underbrace{\Pr\left(a_2\rho_S|h_{Rn^*}|^2 > \vartheta|h_E|^2+\omega_2\right)}_{D}\underbrace{\Pr\left(a_2\rho_R|h_{U_2}|^2 > \vartheta|h_E|^2+\omega_2\right)}_{E} \end{aligned} \tag{29}$$

where $\vartheta = 2^{2R_2}a_2\rho_E$ and $\omega_2 = 2^{2R_2}-1$.

After several steps, P_2^{SOP} can be obtained as (30).

$$\begin{aligned} P_2^{SOP} =& 1-\frac{\lambda_{U_2}e^{-\frac{\omega_2\bar{b}}{\lambda_{U_2}}}}{\vartheta\bar{b}\lambda_E+\lambda_{U_2}}\left[\left(1-e^{-\frac{\rho_I}{\bar{\rho}_S\lambda_{SP}}}\right)\sum_{n=1}^{N}\binom{N}{n}\frac{\lambda_{SR}(-1)^{n-1}e^{-\frac{n\bar{a}\omega_2}{\lambda_{SR}}}}{(\lambda_{SR}+n\lambda_E\bar{a}\vartheta)}\right. \\ &\left.+\sum_{n=1}^{N}\binom{N}{n}\frac{\lambda_{SR}(-1)^n}{\lambda_E\tilde{a}\vartheta\lambda_{SP}n}e^{-\frac{\rho_I}{\bar{\rho}_S\lambda_{SP}}-\frac{n\tilde{a}\rho_I\omega_2}{\bar{\rho}_S\lambda_{SR}}+\varphi_n\Delta_n}Ei\left(-\varphi_n\Delta_n\right)\right] \end{aligned} \tag{30}$$

Let $\rho_S \to \infty$, the error floor $P_2^{SOP,\infty}$ is given by (31).

$$P_2^{SOP,\infty} = 1-\sum_{n=1}^{N}\binom{N}{n}\frac{\lambda_{SR}(-1)^n}{\lambda_E\tilde{a}\vartheta\lambda_{SP}n}e^{\frac{\Delta_n}{\lambda_E}}Ei\left(-\frac{\Delta_n}{\lambda_E}\right) \tag{31}$$

4. NUMERICAL RESULTS

We set main parameters as: power allocation factor $a_1 = 0.9$ and target rates $a_2 = 0.1$. $R_1 = R_2 = 1$. SNR of interference from primary network $\rho_I = 15\,dB$. SNR of eavesdropper $\rho_E = 1\,dB$. The channel gains are $\lambda_{SP} = 0.1$, $\lambda_{SR} = 1$, $\lambda_{RD1} = 0.9$, $\lambda_{RD2} = 0.6$ and $\lambda_{RE} = 0.1$. $Q = V = 1000$. Figure 2 shows SOP performance versus transmit SNR.

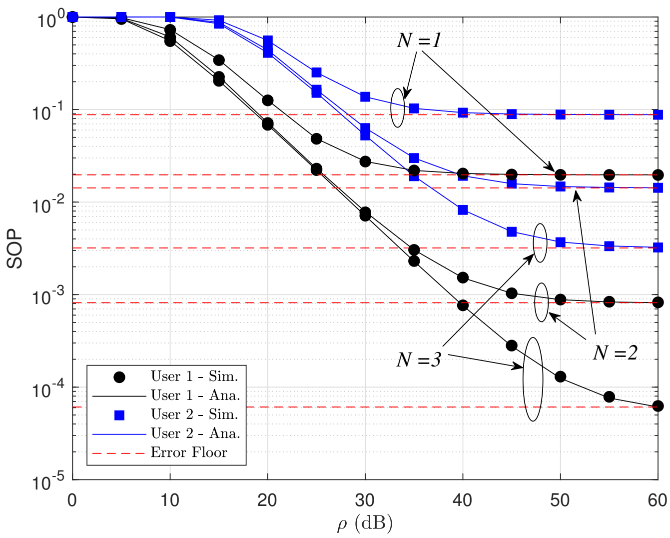

Figure 2. SOP versus transmit SNR at BS

We consider many cases related to NOMA, OMA. As can be seen from such outage performance, the error floor curves are very matched with exact curves at high ρ. Signal x_1 exhibits better SOP compared with x_2, and it can be explained that different power allocated to each signal. The simulation results are also very tight with the analytical results. Similar trend of SOP can be reported in Figure 3. Figure 3 depicts SOP curves versus ρ_I. When ρ_I is greater than 30 (dB), SOP curves meet saturation.

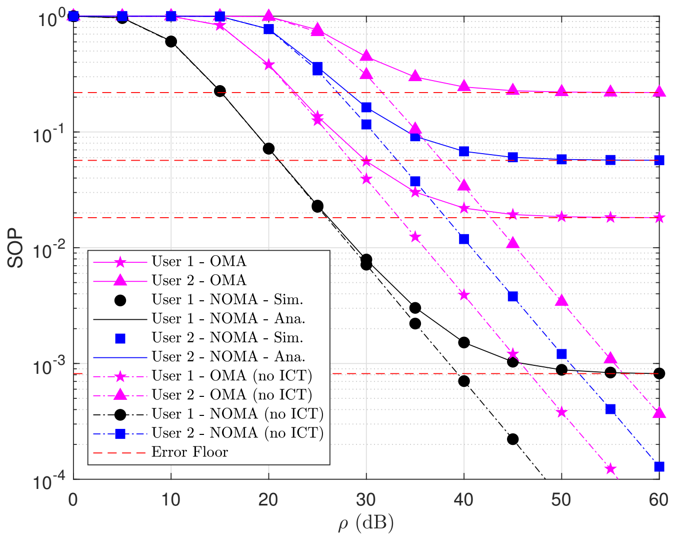

Figure 3. SOP versus transmit SNR at BS

5. CONCLUSION

The paper studied cognitive radio using NOMA and relay selection. Secure performance is considered as existence of an eavesdropper. Moreover, the exact SOP is derived for two destinations. The derivations and analysis results showed that the proposed relay selection can effectively enhance the secure performance.

REFERENCES

[1] T.-T Nguyen, M.-N. Pham, and D.-T. Do, "Wireless powered underlay cognitive radio network with multiple primary transceivers: Energy constraint, node arrangement, and performance analysis," *International Journal of Communication Systems*, vol. 30, no. 18, 2017, doi: 10.1002/dac.3372.

[2] F. Fang, H. Zhang, J. Cheng, S. Roy, and V. C. M. Leung, "Joint user scheduling and power allocation optimization for energy-efficient NOMA systems with imperfect CSI," *IEEE J. Sel. Areas Commun.*, vol. 35, no. 12, pp. 2874-2885, Dec. 2017.

[3] I. Kakalou, K. E. Psannis, P. Krawiec, and R. Badea, "Cognitive radio network and network service chaining toward 5G: Challenges and requirements," *IEEE Commun. Mag.*, vol. 55, no. 11, pp. 145-151, Nov. 2017, doi: 10.1109/MCOM.2017.1700086.

[4] H. Zhang, C. Jiang, X. Mao, and H. H. Chen, "Interference-limited resource optimization in cognitive femtocells with fairness and imperfect spectrum sensing," *IEEE Trans. Veh. Technol.*, vol. 65, no. 3, pp. 1761-1771, Mar. 2016, doi: 10.1109/TVT.2015.2405538.

[5] H. Zhang, Y. Nie, J. Cheng, V. C. M. Leung, and A. Nallanathan, "Sensing time optimization and power control for energy efficient cognitive small cell with imperfect hybrid spectrum sensing," *IEEE Trans. Wireless Commun.*, vol. 16, no. 2, pp. 730-743, Feb. 2017, doi: 10.1109/TWC.2016.2628821.

[6] W. Liang, S. X. Ng, and L. Hanzo, "Cooperative overlay spectrum access in cognitive radio networks," *IEEE Commun. Surveys Tuts.*, vol. 19, no. 3, pp. 1924-1944, 2017, doi: 10.1109/COMST.2017.2690866.

[7] F. Jasbi and D. K. C. So, "Hybrid overlay/underlay cognitive radio network with MC-CDMA," *IEEE Trans. Veh. Technol.*, vol. 65, no. 4, pp. 2038-2047, Apr. 2016, doi: 10.1109/TVT.2015.2417195.

[8] B. Kumar and S. Prakriya, "Performance of adaptive link selection with buffer-aided relays in underlay cognitive networks," *IEEE Trans. Veh. Technol.*, vol. 67, no. 2, pp. 1492-1509, Feb. 2018, doi: 10.1109/TVT.2017.2761990.

[9] P.-M. Nam, D.-T. Do, T.-T. Nguyen, and P. T. Tin, "Energy harvesting assisted cognitive radio: random location-based

transceivers scheme and performance analysis," *Telecommunication Systems*, vol. 67, no. 1, pp. 123-132, 2018, doi: 10.1007/s11235-017-0325-0.

[10] Dinh-Thuan Do and M.-S. Van Nguyen, "Device-to-device transmission modes in NOMA network with and without wireless power transfer," *Computer Communications*, vol. 139, pp. 67-77, May 2019.

[11] D.-T. Do, M. Vaezi, and T.-L. Nguyen, "Wireless powered cooperative relaying using NOMA with imperfect CSI," in *Proc. of IEEE Globecom Workshops (GC Wkshps)*, Abu Dhabi, UAE, pp. 1-6, 2018.

[12] Do D-T, Le C-B, and Lee BM, "Robust transmit antenna design for performance improvement of Cell-Edge users: Approach of NOMA and Outage/Ergodic Capacity Analysis," *Sensors*, vol. 19, no. 22, 2019.

[13] D.-T. Do and A.-T. Le, "NOMA based cognitive relaying: Transceiver hardware impairments, relay selection policies and outage performance comparison," *Computer Communications*, vol. 146, pp. 144-154, 2019.

[14] D.-T. Do, A.-T. Le, and B.-M. Lee, "On performance analysis of underlay cognitive radio-aware hybrid OMA/NOMA networks with imperfect CSI," *Electronics*, vol. 8, no. 7, 2019, doi: 10.3390/electronics8070819.

[15] Dinh-Thuan Do, M.-S. Van Nguyen, T.-A. Hoang, and M. Voznak, "NOMA-Assisted multiple access scheme for IoT deployment: Relay selection model and secrecy performance improvement," *Sensors*, vol. 19, no. 3, 2019, doi: 10.3390/s19030736.

[16] C. Dang, L. Jimenez-Rodrıguez, N. H. Tran, S. Shetty, and S. Sastry, "On secrecy rate and optimal power allocation of the full-duplex amplify-and-forward relay wire-tap channel," *IEEE Trans. on Vehic. Tech.*, vol. 66, no. 5, pp. 3887-3899, May 2017, doi: 10.1109/TVT.2016.2600658.

[17] B. M. ElHalawany, R. Ruby, T. Riihonen, and K. Wu, "Performance of cooperative NOMA systems under passive eavesdropping," in *Proc. IEEE GLOBECOM*, pp. 1-6, Dec. 2018.

[18] N. Yang, H. A. Suraweera, I. B. Collings, and C. Yuen, "Physical layer security of TAS/MRC with antenna correlation," *IEEE Trans. Inform. Forensics and Security*, vol. 8, no. 1, pp. 254-259, Jan. 2013, doi: 10.1109/TIFS.2012.2223681.

[19] M. Zhang and Y. Liu, "Energy harvesting for physical-layer security in OFDMA networks," *IEEE Trans. Inform.n Forensics and Security*, vol. 11, no. 1, pp. 154-162, Jan. 2016, doi: 10.1109/TIFS.2015.2481797.

[20] D. Tubail, M. El-Absi, S. S. Ikki, W. Mesbah, and T. Kaiser, "Artificial noise-based physical-layer security in interference alignment multipair two-way relaying networks," *IEEE Access*, vol. 6, pp. 19073-19085, 2018, doi: 10.1109/ACCESS.2018.2817264.

[21] Y. Zou, X. Wang, and W. Shen, "Physical-layer security with multiuser scheduling in cognitive radio networks," *IEEE Trans. Commun.*, vol. 61, no. 12, pp. 5103-5113, Dec. 2013.

[22] Y. Jiang, J. Ouyang, and Y. Zou, "Secrecy energy efficiency optimization for artificial noise aided physical-layer security in cognitive radio networks," in *Proc. IEEE ITU K*, Nov. 2017, pp. 1-6.

[23] F. Zhou, Z. Chu, H. Sun, R. Q. Hu, and L. Hanzo, "Artificial noise aided secure cognitive beamforming for cooperative miso-noma using swipt," *IEEE J. Sel. A. Commun.*, vol. 36, no. 4, pp. 918-931, Apr. 2018, doi: 10.1109/JSAC.2018.2824622.

[24] Y. Zhang, H. M. Wang, Q. Yang, and Z. Ding, "Secrecy sum rate maximization in non-orthogonal multiple access," *IEEE Commun. Let.*, vol. 20, no. 5, pp. 930–933, May 2016, doi: 10.1109/LCOMM.2016.2539162.

[25] G. He, L. Li, X. Li, W. Chen, L. L. Yang, and Z. Han, "Secrecy sum rate maximization in noma systems with wireless information and power transfer," in *Proc. WCSP*, pp. 1-6, Oct. 2017.